HIGH-RESOLUTION, MULTIPLE OPTICAL MODE CONFOCAL MICROSCOPE: II. THEORETICAL ASPECTS OF CONFOCAL TRANSMISSION MICROSCOPY

*Kieran G. Larkin, Carol J. Cogswell, John W. O'Byrne, and Matthew R. Arnison
Department of Physical Optics, School of Physics, University of Sydney, NSW 2006, AUSTRALIA

ABSTRACT

Much analysis of microscope image formation is based upon the so-called weak scattering approximation in which an image is linearly related to an object by a convenient convolution property which greatly simplifies reconstruction. This approximation is often invalid in transmission microscopy.

A better model of transmission must account for multiple scattered components in the light distribution. In the simplest embodiment of such a model the object is represented by a 3-D optical density distribution. Light transmitted through such an object is related to the total density along a ray path. Consequently the imaging process can be linearized by a logarithmic transform of the transmitted light distribution. Once linearized, conventional deconvolution techniques can be applied to a surface integral of the transformed intensity. Surprisingly this logarithmic model of imaging predicts a power series expansion representing the 3-D attenuation distribution. The first term is related to the confocal image, the second term corresponds to the conventional image.

Implications of this multiplicative approach to image reconstruction are explored. The model also predicts critical parameters of the so-called "wandering" spot and may be useful in determining the optimum tracking criteria in a transmission confocal microscope incorporating adaptive optical technologies.

INTRODUCTION

This paper consists of four main sections. Following the introduction, Section 1 presents salient features of the two main approximations used to model propagation of light through inhomogeneous media. Section 2 develops a multiplicative model of transmission through a specimen using a geometric ray formulation. Section 3 extends the results obtained from the preceding section to demonstrate the relation between multiplicative imaging and both confocal and conventional imaging. Section 4 discusses some implications of image reconstruction using the multiplicative model.

The aim of this paper is to explore the implications of a multiplicative model of optical imaging. Most previous work on confocal transmission imaging has been based upon an additive imaging process. The question of the validity of either theory is not considered in detail here but interested readers should consult recent work comparing the two[1, 2].

1. ESSENTIAL BACKGROUND

Although several authors have performed confocal transmission microscopy of various semi-transparent samples [3-9], the relationship between the resulting transmission image and the original object is not clear. In the case of double-pass transmission confocal microscopy [7, 9], the system symmetry ensures that (for small phase inhomogeneities at least) the irradiance distribution falling upon the confocal pinhole detector remains correctly centred , as indeed it does in the reflection and epi-fluorescence modes of a confocal microscope. However, the single-pass confocal configuration produces an irradiance distribution upon the detector plane which can "wander" significantly from the nominal centre of the system . Aspects of this wandering have been described by O'Byrne and Cogswell [10, 11].

It should be noted that the de-scanning optics described by Dixon [6] only compensates the beam tilt due to the image scanning system and *not* tilts due to specimen refractive index variations. Rigorous analysis of transmission microscopy is fraught with difficulties. Much of the analysis performed so far has assumed some simplifying approximations. Frequently the weak scattering theory is used where the solution is given by the first Born approximation [12-14]. The essence of this approximation is that the scattered field from any one plane of the specimen is unaffected by scattering in any other plane. In other words the field is considered to be scattered once, at most. Clearly this conclusion is untenable for many typical specimen types: the light transmitted through a particular region is certain to have affected its transmission through other regions.

An alternative approach - which is known as the Rytov approximation [see, for example, Ishimaru[1, 15]] - includes some affects of multiple scattering. The Born and Rytov models produce fundamentally different results

which are best illustrated by a simple example: Consider the light transmitted through two neutral density filters of transmittances, T_1 and T_2. The first Born approximation predicts the overall transmittance, T_B to be as follows

$$T_B = T_1 + T_2 - 1 \tag{1}$$

Whereas the Rytov approximation predicts an overall transmittance T_R, where

$$T_R = T_1 T_2 \tag{2}$$

If $T_1 = T_2 = 0.5$, then $T_R = 0.25$ and $T_B = 0.0$. Thus we can conclude - for this grossly simplified case - that the Born approximation gives poor results for specimens with transmissions of the order 0.5 and lower.

2. MULTIPLICATIVE MODEL OF TRANSMISSION THROUGH SPECIMEN

The following analysis will only consider a purely absorbing specimen which has a constant refractive index throughout. Thus phase effects (refraction) may be ignored. However, rather than develop the Rytov approach for transmission microscopy, which can be expected to be a lengthy process, we shall instead consider a simplified model which, nevertheless, illustrates important aspects of the Rytov (or, rather, the multiplicative method). An extension to weakly varying refractive index is possible but beyond the scope of this paper [16-18]. For convenience geometrical propagation of light rays is assumed. However, it can be shown that a simple modification using quadratic phase factors can extend the theory so that diffraction effects are included. Again such an extension will not be considered here as it does not alter the main conclusions drawn from the model.

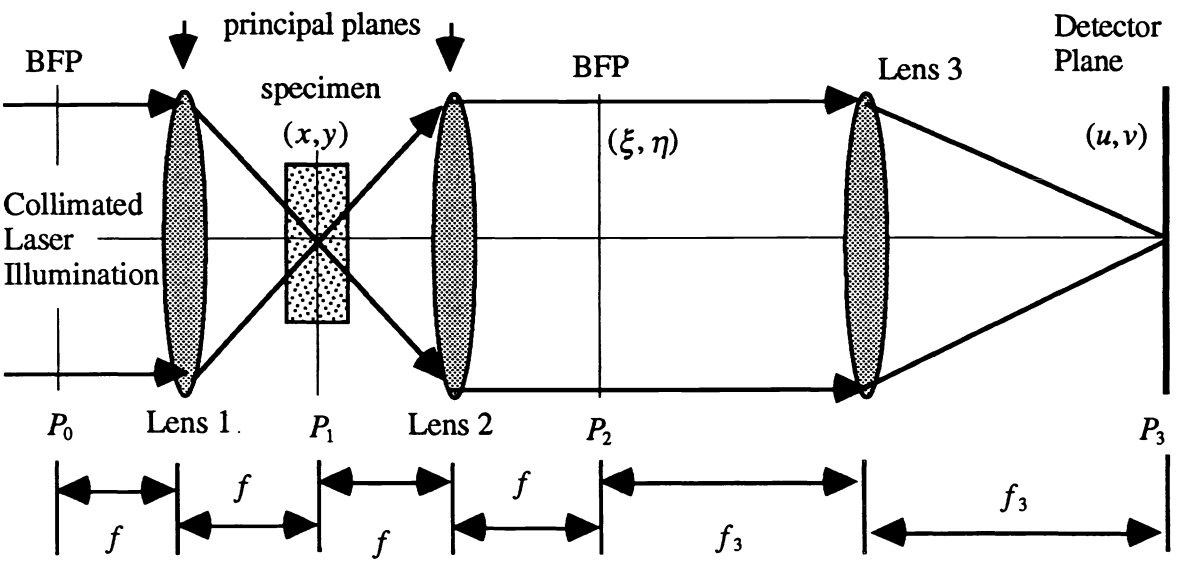

Figure 1: Confocal transmission configuration

Consider the optical configuration in Figure 1. A specimen is placed between two matched objectives which are spaced such that they have coincident focal planes within the specimen. The optical system is axially symmetric with the exception of the specimen which may have an arbitrary distribution of transmittance. To satisfy, strictly, conditions

required for geometric ray tracing, the transmittance distribution must have spatial variations which occur over distances much larger than the wavelength of light used to probe the specimen. Such a condition will be assumed initially. A uniform collimated quasimonochromatic beam enters the back focal plane of the illuminating object (L_1). The light is focused down into the specimen and the emerging light is collected by objective (L_2) and collimated so that a plane wavefront with a specimen-modulated amplitude emerges at the second back focal plane P_2. For simplicity the specimen refractive index is assumed to be matched to the index of the medium in the focal region of the two objectives.

A light ray entering the specimen with amplitude U_1 is progressively absorbed as it transverses in a straight line path. The well-known concept of optical density can be utilised to generate a simple expression for the amplitude of the ray emerging from the specimen. A closely related idea is used in computer tomography [19-23]. For convenience our definition of optical density will use natural logarithms as opposed to logarithms base 10 used conventionally. If the (amplitude) transmittance is τ then

$$\tau = e^{-\text{Density}} \tag{3}$$

A uniform absorbing medium has an optical density directly proportional to its thickness (which relates to the path taken by transmitted light). A non uniform purely absorbing medium will have an overall density related to the path integral of its local density function

$$\tau = \exp -\left(\int \rho \, d\ell\right) \tag{4}$$

where $\rho = \rho(x,y,z)$ is the local density function of the specimen. The units of ρ are reciprocal length, that is to say optical density per metre. The convenience afforded by this optical density approach is apparent in the above equation where the total transmittance is equated to an additive quantity (in this limit the summation becomes an integral).

As an intermediate step in the modelling it is necessary to evaluate the beam amplitude U_1 in the back focal plane P_1. Consider the details of ray transmission through the specimen in Figure 2. The field strength associated with the incoming ray is U_0 and is assumed to be constant over the lens aperture. the path length along the ray is inversely proportional to $\cos\theta$, where θ is the ray-axis angle. The path integral in Eq.4 can be rewritten

$$U_1 = U_0 \exp\left\{-\frac{1}{\cos\theta}\iiint \rho(x,y,z)\delta(x-\xi z/f)\delta(x-\eta z/f)b(z)dxdydz\right\} \tag{5}$$

The Dirac delta function selects only those points on the path, whilst the rectangular function $b(z)$ limits the range of the integration with respect to z. The parameter Z is just the objective focal length (that is to say the path length is limited to the region between the two lenses).

$$b(z) = \begin{cases} 1, for|z| < Z \\ 0, otherwise \end{cases} \tag{6}$$

Now an expression for the normalized outgoing field can be derived

$$\ln\left(\frac{U_1(\xi,\eta)}{U_0}\right) = -\frac{1}{\cos\theta}\int \rho(\xi z/f, \eta z/f, z)b(z)dz \tag{7}$$

Equation 7 is valid at all points in the BFP P_1 (because of the geometrical approach here the amplitude is unaltered between the lens principal plane and P_1).

The next step is to evaluate the integral of the logarithmic amplitude over the rear stop of the objective (in the plane P_1). The reason for this type of integral will become apparent later. At this point we must assume that there are

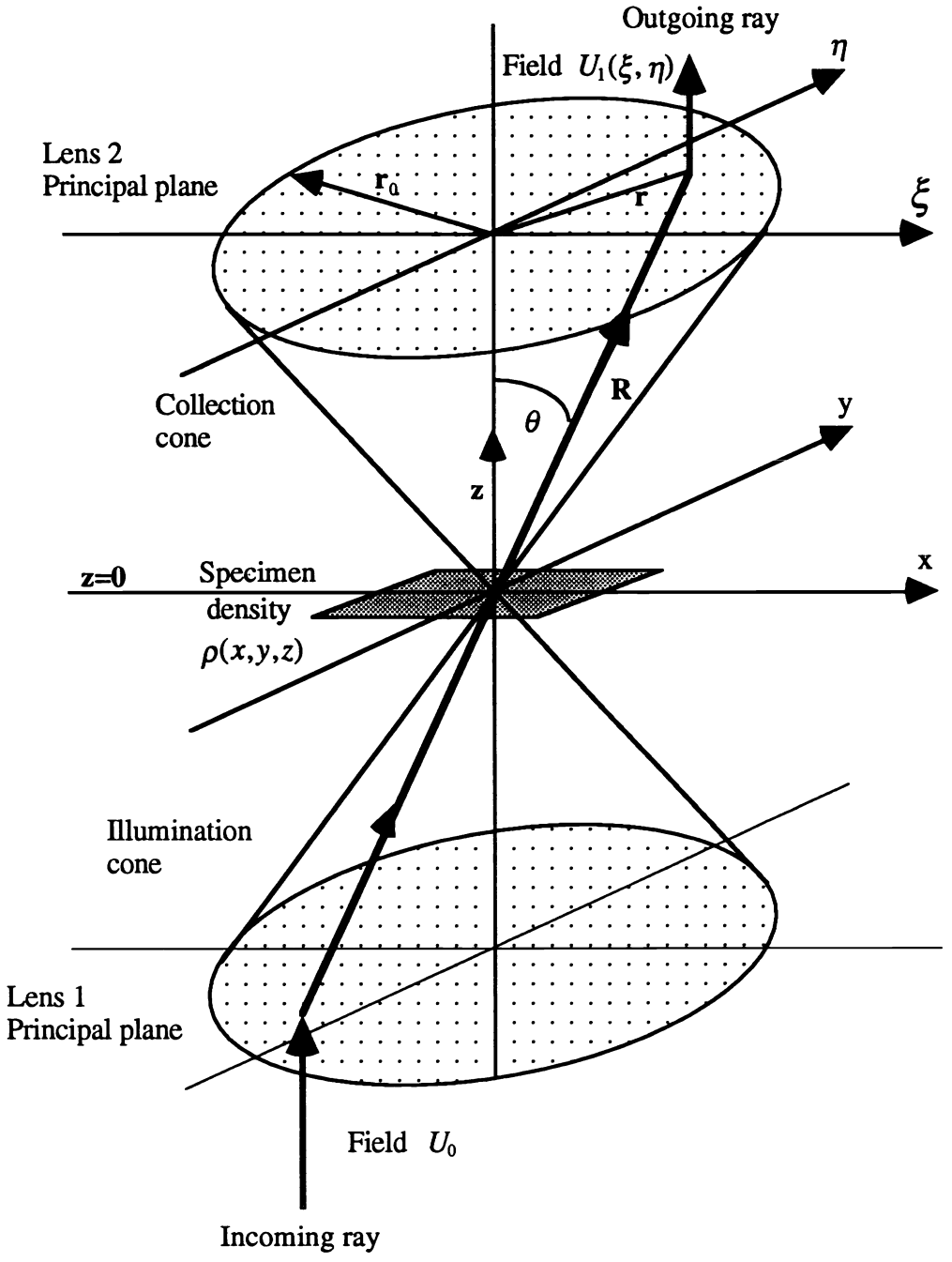

Figure 2: Details of transmission geometry

no opaque regions in the specimen, otherwise the amplitude can drop to zero and hence the logarithm approaches (minus) infinity. Physically this corresponds to the fact that opaque regions shadow other regions and prevent that regional information from emerging from the specimen. This transmission model breaks down for specimens with opaque regions and suggests that, in general, imaging of such specimens involves the unavoidable loss of shadow region information.

The integral I is defined as follows

$$I = \iint_S \ln\left(\frac{U_1(\xi,\eta)}{U_0}\right) d\xi d\eta \tag{8}$$

where S defines the surface area of the objective rear stop. A corresponding aperture function $a(\xi,\eta)$ can be defined for this surface ($\xi^2 + \eta^2 = r^2$)

$$a(\xi,\eta) = \begin{cases} 1, for |r| < r_0, \\ 0, otherwise \end{cases} \tag{9}$$

Consequently

$$I = -\iint \frac{a(\xi,\eta)}{\cos\theta} \left\{ \int \rho(\xi z/f, \eta z/f, z) b(z) dz \right\} d\xi d\eta \tag{10}$$

Changing the order of integration and noting that $x = \xi f/z$ and $y = \eta f/z$

$$I = -\iiint \rho(x,y,z) \left[\frac{a(\xi,\eta) b(z)}{\cos\theta(\xi,\eta)} \frac{f^2}{z^2} \right] dx dy dz \tag{11}$$

After some manipulation I can be rewritten

$$I = -\iiint \rho(x,y,z) . p(x,y,z) \mathrm{d}x\mathrm{d}y\mathrm{d}z \tag{12}$$

If the specimen is shifted from the origin to a point (x_0, y_0, z_0) the integral clearly becomes a convolution

$$I(x_0,y_0,z_0) = -\iiint \rho(x-x_0, y-y_0, z-z_0) p(x,y,z) . \mathrm{d}x\mathrm{d}y\mathrm{d}z \tag{13}$$

Thus $p(x,y,z)$ represents the geometric point spread function (PSF) for multiplicative imaging. The function p defines a double conical region (identical to the illumination and collection cones) with a weighting function which accounts for the $1/\cos\theta$ path length through the specimen as well as the $1/z$ blur circle amplitude.

In this section we have shown that a measurement of the surface integral of logarithmic field isolates the blurred 3-D distribution of the optical density function ρ. However to recover the distribution a deconvolution must be performed. The convolution kernel in this instance is p, a double conical function. Fourier analysis of p shows the well known "missing cone" of spatial frequencies [8, 14, 24, 25]. It is thus inevitable that measurements of the integral I contain no information about certain spatial frequencies present in ρ. This is not a particularly surprising result and fits in well with previous work which uses the Born approximation. The real importance of the model developed in this chapter is that the 3-D *optical density* distribution can, in principle, be recovered *exactly* (apart from the missing cone).

A recent paper by Wu & Schwarzman[26] developed a similar multiplicative theory but applied the process to measurements taken in the image plane of a conventional microscope, whereas the system we propose uses coherent

illumination with a confocal arrangement of illuminating and collecting objectives.

3. CORRESPONDENCE BETWEEN MULTIPLICATIVE IMAGING AND BOTH THE CONFOCAL AND CONVENTIONAL IMAGES

In the previous section we derived an expression for the field amplitude in the back focal plane of the collecting objective (see plane P_2 in Figure 1). The relationship can be written

$$U_1 = U_0 \exp -\{\rho * p\} \tag{14}$$

where * indicates convolution. Although the analysis so far has utilized the geometrical optics approach, the above equation can be modified to satisfy the wave theory approach merely be replacing p with p_D which contains a quadratic (defocus) phase factor.

The field at P_2 is Fourier transformed by lens 3 to give the field at the detector plane P_3. Two important Fourier transform properties will be shown to have important repercussions for both conventional and confocal imaging. Definitions of both modes of imaging will be given at the relevant points of the analysis.

If the field amplitude in plane P2 is $h(\xi,\eta)$ then the field in plane P3 is $H(u,v)$ where:

$$H(u,v) = A\iint h(\xi,\eta)\exp(-2\pi i[u\xi + v\eta])d\xi d\eta \tag{15}$$

The above expression is merely the Fraunhofer diffraction integral. The coefficient A is related to radiation wavelength λ, and lens focal length f. The co-ordinates u and v are scaled relative to λ and f_2. Details of the above transform relation are given by Goodman [27] for example. The field at the origin of plane P3 is just $H(0,0)$ with

$$H(0,0) = A\iint h(\xi,\eta)d\xi d\eta \tag{16}$$

In other words, the quantity $H(0,0)$ is directly related to the surface integral of the field h at the plane P2 (the BFP of objective lens L2). If a small pinhole is placed at O3 the signal, C, detected by a detector behind the pinhole will be directly proportional to $|H(0,0)|^2$. The radius of the pinhole must be substantially smaller than the radius of the first zero ring of the diffraction pattern formed when the system contains a clear (reference) specimen. In this case C corresponds to the transmission brightfield confocal signal.

A signal which can be easily measured is the total power, T, reaching the detector plane.

$$T = \iint |H(u,v)|^2 \, dudv \tag{17}$$

By Rayleigh's theorem (see, for example, Bracewell [28]) this can be shown to be

$$T = \iint |h(\xi,\eta)|^2 \, d\xi d\eta \tag{18}$$

It can also be shown that T corresponds to the conventional (non-confocal) transmission brighfield image. To summarize this section so far: the total integrated field at the BFP P2 is proportional to the square root of the confocal image, whilst the total integrated irradiance of BFP P2 is proportional the conventional image.

Now consider the quantity I defined in the previous section, equation (8). If the absorption in the specimen is not too great, then the logarithm in the integrand may be expended as a power series. Let $U_1/U_0 = 1 - g(\xi,\eta)$, then

$$I = -\iint_S \ln(1-g)\,d\xi d\eta = -\iint_S \left(g + \frac{g^2}{2} + \frac{g^3}{3} \right) d\xi d\eta \tag{19}$$

The first two terms of the series give the second order approximation which has less than 10% error for values of absorption g less than 0.6. Defining I_2 as the second order approximation leads to

$$I_2 = -\iint_S \left(g + \frac{g^2}{2} \right) d\xi d\eta = -\frac{1}{2} \iint_S \left(3 - 4\frac{U_1}{U_0} + \frac{U_1^2}{U_0^2} \right) d\xi d\eta \tag{20}$$

The rightmost integral above consists of three parts: the first is just a constant, the second is the normalised (square root) confocal image, the third is the normalised conventional image. Explicitly

$$I_2 = -\frac{1}{2} \left(3 - 4\sqrt{\frac{C}{C_0}} + \frac{T}{T_0} \right) \tag{21}$$

where C_0 is the confocal image signal for a clear specimen, and T_0 is the conventional image signal for a clear specimen.

In this section we have demonstrated an important point: that the information necessary to reconstruct the 3-D density distribution can be approximated by a composite data set constructed from the confocal and the conventional images. Composite images have been used previously to sharpen axial response in refection imaging [29], but not for the improvement of image fidelity in transmission microscopy.

4. IMPLICATIONS OF THE MULTIPLICATIVE MODEL

The multiplicative model developed so far allows the 3-D optical density distribution to be estimated by the following process:

i) sample the conventional image over a 3-D array of points
ii) simultaneously sample the confocal image over same array
iii) combine the arrays to generate a composite image [Eq.(21)]
iv) deconvolve using a known PSF p [where $I_2 \approx \rho * p$]
v) optionally transform back to transmittance using Eq.(3)

The end result is expected to have greater image fidelity than either the deconvolved conventional or deconvolved confocal arrays. In part I of this paper the multiple optical mode microscope was used to collect 3-D datasets of chromosomes (from an orchid root tip) in transmission and transmission Nomarski. The process outlined above in steps i) to v) has not yet been applied in full. Preliminary results up to step iii) indicate that the composite image is visually rather similar to both of its basis images. Spatial frequency analysis shows a broadly similar image power spectrum. However, other indictors such as intensity histograms look quite different. The crucial test of the models validity is whether or not it reduces artifacts in the deconvolved image.

In both sections 2 and 3 the phase changes in the wavefront have been assumed to be uniform across the aperture (the optical path of all rays is considered constant). A direct consequence of this is that the irradiance distribution upon the detector plane has 180 degree rotational symmetry, hence the irradiance centroid is always located on axis. Conveniently this allows us to sample the confocal image with a fixed pinhole. If, however, the phase is non-uniform, then the centroid may occur off-axis. The exact location of the centroid is then dependent upon the overall phase symmetry. Initial analysis of the phase effects indicate that the irradiance level in the region of the centroid carries the information necessary for image reconstruction. Consequently a transmission confocal microscope for phase and amplitude (absorption) imaging system may need to track the wandering spot centroid.

CONCLUSION

A multiplicative theory of optical imaging has been developed and the major implications of such a theory for image acquisition and reconstruction have been explored. The concept of a composite image with improved image fidelity has been introduced. Experimental confirmation of the model's applicability is now required.

ACKNOWLEDGEMENTS

The authors would like to thank Colin Sheppard for many enlightening discussions about the scattering of light in specimens. We would also like to thank Richard Piorkowski for invaluable assistance building the microscope and Kerwyn Foo for preliminary analysis and assesment of the composite images.

The Physical Optics Department is supported by funds from the University of Sydney, the Science Foundation for Physics within the University of Sydney, and the Australian Research Council.

REFERENCES

1. Kaveh, M., and Soumekh, M., "Computer-Assisted Diffraction Tomography," 369-413, Image Recovery: Theory and Application, ed. Henry Stark., Academic Press, Orlando, 1987.
2. Lin, E. C., and Fiddy, M. A., "The Born-Rytov controversy: I. Comparing analytical and approximate expressions for the one-dimensional deterministic case," Journal of the Optical Society of America, **9**,(7), 1102-1110, (1992).
3. Brakenhoff, G. J., "Imaging modes in confocal scanning light microscope (CLSM)," Journal of Microscopy, **117**, 223-242, (1979).
4. Cogswell, C. J., and Sheppard, C. J. R., "Imaging using confocal brightfield techniques," EMAG-MICRO 89, Vol. (London: IOP, 1989).
5. Sheppard, C. J. R., and Cogswell, C. J., "Reflection and transmission confocal microscopy," First International Conference on Optics Within Life Sciences, Vol.**1**, 310-315 (Garmisch-Partenkirchen: Elsevier, 1990).
6. Dixon, A. E., Damaskinos, S., and Atkinson, M. R., "Transmission and double-reflection scanning stage confocal microscope," Scanning, **13**, 299-306, (1990).
7. Sheppard, C. J. R., and Wilson, T., "Multiple travesing of the object in the scanning microscope," Optica Acta, **27**,(5), 611-624, (1980).
8. Sheppard, C. J. R., and Cogswell, C. J., "Three-dimensional Imaging in Confocal Microscopy," 143-169, Confocal Microscopy, ed. T. Wilson. Academic Press, 1990,
9. Cogswell, C. J., and Sheppard, C. J. R., "Confocal Brightfield Imaging Techniques Using an On-Axis Scanning Optical Microscope," 213-242, Confocal Microscopy, ed. T. Wilson. Academic Press, 1990,
10. Cogswell, C. J., and O'Byrne, J. W., "A high resolution confocal transmission microscope: I. System design," SPIE conference on Biomedical Image Processing and Three-Dimensional Microscopy, Vol.**1660**, 503-511 (San Jose: SPIE, 1992).
11. O'Byrne, J. W., and Cogswell, C. J., "A high resolution confocal transmission microscope: II. Determining image position and correcting aberrations," SPIE conference on Biomedical Image Processing and Three-Dimensional Microscopy, Vol.**1660**, 512-520 (San Jose: SPIE, 1992).
12. Born, M., and Wolf, E., Principles of Optics, Pergammon Press, Oxford, 1965.
13. Wolf, E., "Three-dimensional structure determination of semi-transparent objects from holographic data," Optics Communications, **1**,(4), 153-156, (1969).
14. Streibl, N., "Three-dimensional imaging by a microscope," Journal of the Optical Society of America, A, **2**,(2), 121-127, (1985).
15. Ishimaru, A., Wave Propagation and Scattering in Random Media, Academic Press, New York, 1978.
16. Sasaki, O., and Kobayashi, T., "Beam-deflection optical tomography of the refractive-index distribution based on the Rytov approximation," Applied Optics, **32**,(5), 746-751, (1993).
17. Lira, I. H., and Vest, C. M., "Refraction correction in holographic interferometry and tomography of transparent objects," Applied Optics, **26**,(18), 3919-3929, (1987).
18. Noda, T., Kawata, S., and Minami, S., "Three-dimensional phase-contrast imaging by a computed-tomography microscope," Applied Optics, **31**,(5), 670-674, (1992).

19. Bates, R. H. T., and McDonnell, M. J., Image Restoration and Reconstruction, Clarendon Press, Oxford, 1986.
20. Andersen, A. H., "Tomography transform and inverse in geometrical optics," Journal of the Optical Society of America, A, **4**,(8), 1385-1395, (1987).
21. Maleki, M. H., Devaney, A. J., and Schatzberg, A., "Tomographic reconstruction from optical scattered intensities," Journal of the Optical Society of America, A, **9**,(8), 1356-1363, (1992).
22. Verhoeven, D., "Multiplicative algebraic computed tomographic algorithms for the reconstruction of multidimensional interferometric data," Optical Engineering, **32**,(2), 410-, (1993).
23. Brown, C. S., et al., "Computed tomography from optical projections for three-dimensional reconstruction of thick objects," Applied Optics, **31**,(29), 6247-6254, (1992).
24. Sheppard, C. J. R., and Gu, M., "The significance of 3-D transfer functions in confocal scanning microscopy," Journal of Microscopy, **165**,(3), 377-390, (1992).
25. Sheppard, C. J. R., "General considerations of diffraction theory of 3-D imaging," European Journal of Cell Biology, **48**,(Suppl. 25), 29-32, (1989).
26. Wu, X., and Schwarzmann, P., "Nonlinear approach to the 3D-reconstruction of microscopic objects," Biomedical Image Processing II, Vol.**1450**, 278-285 (SPIE, 1991).
27. Goodman, J. W., Introduction to Fourier optics, McGraw-Hill, San Francisco, 1968.
28. Bracewell, R. N., The Fourier transform and its applications, McGraw Hill, New York, 1978.
29. Sheppard, C. J. R., and Cogswell, C. J., "Confocal microscopy with detector arrays," Journal of Modern Optics, **37**,(2), 267-279, (1990).